Iranian (Iranica) Journal of Energy & Environment
Journal Homepage: www.ijee.net
IJEE an official peer review journal of Babol Noshirvani University of Technology, ISSN:2079-2115

Thermal Analysis of New Solar Air Heater with Inclined Perforated Absorber Plates: Experimental Study

H. Farzan[1]*, M. Mahmoudi[1], E. Hasan Zaim[2]

[1] Mechanical Engineering Department, Faculty of Engineering, Higher Education Complex of Bam, 76615-314, Bam, Iran
[2] Mechanical Engineering Department, Sirjan University of Technology, 78137-33385, Sirjan, Iran

PAPER INFO

Paper history:
Received 29 December 2022
Accepted in revised form 29 January 2023

Keywords:
Perforation method
Perforated solar air heaters
Thermal efficiency
Transient heat dynamics

ABSTRACT

Solar air heaters (SAHs) have an inherent drawback: the conventional mechanism is low inside these collectors' types. Use of perforations is a simple technique to improve convection, and this investigation experimentally assesses a novel design SAH utilizing three inclined perforated absorber plates. Two scenarios are considered to assess the dynamics and efficiency of this perforated SAH, including m_{air} = 0.012 kg/s and 0.024 kg/s. Numerous sensors monitored the dynamics of the perforated SAH and ambient factors for 12 hours in October 2022. The experimental outcomes illustrate that the perforation method remarkably enhances the thermal efficiency of the perforated SAH compared with standard smooth SAHs. The daily thermal efficiency of the perforated SAH reaches 73.30% and 82.65%, while the outlet air temperature experiences peak values of 39 °C and 42 °C at noon and keeps within 90% of its maximum value for 2 hours for the scenarios considered. Improving the convection mechanism causes the flowing air to extract the absorber's thermal energy more effectively. Hence the SAH can produce an airstream near its maximum temperature for an extended duration. In conclusion, the perforation method is a robust, simple method to boost the thermal efficiency of SAHs.

***doi**: 10.5829/ijee.2023.14.02.11*

NOMENCLATURE

A_c	Collector aperture area (m^2)	w	Uncertainty
c_p	Specific heat capacity (J/kg.K)	**Subscript**	
G	Solar Intensity (W/m^2)	*in*	Inlet
$\dot{m}$	Mass flow rate (kg/s)	*out*	Outlet
Q	Heat gain (J)	**Greek Symbols**	
T	Temperature (°C)	$\eta_{I,Daily}$	Daily thermal efficiency
v	Velocity (m/s)		

INTRODUCTION

Nowadays, solar energy has gained significant attention since it is the most sustainable and affordable green energy source [1, 2]. Hence many techniques, such as solar air heaters (SAHs), have been developed to harness incoming thermal solar energy. SAHs are an affordable, applicable, and easy maintenance method utilized in numerous, wide applications, such as heating homes to dry foods. However, SAHs have an inherent drawback: the convection mechanism is weak inside these solar thermal collectors. Many techniques have been suggested and analyzed to address this problem, including using baffles, fins, dimples, and porous materials [2, 3]. Even though these methods improve the thermal efficiency of SAHs, utilizing them requires configurations, size, and arrangement optimizations [4, 5]. Perforations are a robust method to enhance the convective heat exchange

*Corresponding Author Email: hadi.farzan@bam.ac.ir (H. Farzan)

Please cite this article as: H. Farzan, M. Mahmoudi, E. Hasan Zaim, 2023. Thermal Analysis of New Solar Air Heater with Inclined Perforated Absorber Plates: Experimental Study, Iranian (Iranica) Journal of Energy and Environment, 14(2), pp. 189-196. Doi: 10.5829/ijee.2023.14.02.11

rate in heat transfer applications. Perforated SAHs are new design collectors using perforated absorbers instead of conventional ones. The airstream passing inside these collectors passes through holes in absorber plates, which this issue causes the convection heat exchange rate to improve; consequently, the thermal efficiency increases using this simple technique.

Recent investigations mainly focused on using artificial roughness to improve the thermal performance of SAH; however, numerous studies have extended the artificial roughness method by simultaneously utilizing this technique and perforations to maximize thermal performance [6-8]. Vaziri et al. [9] conducted an experimental study to assess the thermal performance of SAHs using perforated metal and plexiglass top covers. The obtained results proved that the transpired SAH using the perforated plexiglass top cover has the highest thermal performance of 85%, while the unglazed metal perforated SAH reaches a thermal performance of 50%. Skullong et al. [10] introduced two perforated and nonperforated winglet-type vortex generators, including rectangular and trapezoidal winglets, installed on absorber plates. They proved that the perforated winglets have a higher performance than the nonperforated ones. The perforation method enhances the heat transfer factor by nearly 6.78 times compared to the smooth-duct SAH; however, using the perforated vortex generators significantly increases the friction factor. Faujdar and Agrawal [11] and Jain et al. [12] investigated the thermal performance of a V-shape perforated-baffled SAH, assessed the effects of baffles relative height ratio on the thermal performance of the SAH, and found the optimum baffles relative height ratio. They concluded that increasing the relative height ratio increases the Nusselt number; however, the friction factor enhances in a steeper gradient than the Nusselt number. Hassan et al. [13] experimentally analyzed double-pass corrugated conventional and perforated SAHs in energy, exergy, and economic aspects. They illustrated that the corrugated perforated SAH has the highest thermal performance of 71.8%, while the conventional corrugated SAH has the lowest thermal performance of 52.5%. Furthermore, the corrugated conventional and corrugated SAHs achieve energy costs of $0.0427 /kWh and $0.0324 /kWh, respectively, which reveals that the perforated SAH has higher energy and economic performances than the conventional one.

Pandey and Kumar [14] studied the installation orientation of the perforated V-baffle blocks on SAHs' absorbers. This study assessed two installation orientations and reported that perforated V-up baffles increase the Nusselt number by 4.556 times compared to smooth-duct SAHs. Using this approach causes the thermal efficiency to reach nearly 91.6%. Khanlari et al. [15] examined the effects of employing perforated baffled/nano-coated absorbers on the thermal efficiency of SAHs. The acquired experimental data illustrated that using the nano-coating strategy improves the thermal efficiency by nearly 4%, while the exergy efficiency increases by 9.25% to 10.58%. Tandel and Modi [16] combined a perforated baffled SAH with a solar water heater (SWH) and constructed an augmented SAH. The results illustrated that the augmented SAH has 17.1% and 27.28% higher daily thermal efficiency than conventional SAHs and SWHs.

However, compared to the perforated artificial roughness method, a few studies analyzed utilizing perforated absorbers thermally [17, 18]. Mahmood [19] evaluated the thermal performance of a new double-pass perforated SAH using packing wire mesh layers. This experimental study assessed the effects of ambient and operational conditions on the efficiency of the SAH. The experimental outcomes demonstrated that this approach causes the thermal efficiency and temperature difference to reach 86% and 38.6 ^{o}C. Shetty et al. [20, 21] introduced and analyzed a cross-flow solar heater with a circular perforated absorber to improve the weak convection heat mechanism. The acquired experimental data illustrated that the thermohydraulic performance increases by enhancing the diameter and number of the perforations; however, the thermal efficiency reduces marginally in these conditions. Furthermore, they reported a maximum thermal efficiency of 75.55%, choosing the optimum number and diameter of perforations. Arunkumar et al. [22, 23] assessed the dynamics and performance of a double-pass SAH using a rectangular perforated absorber. This collector uses a varying height configuration that allows the inlet air to split between two air channels inside the SAH. The performed numerical and experimental analyses proved that the diameter and number of perforations affect the thermohydraulic performance. The peak reported thermal and hydrothermal efficiencies were 81.06% and 84.8%, respectively, selecting a height ratio of 0.66.

As discussed in the literature review, the recent study mainly emphasizes using perforated artificial roughness in different configurations installed on absorbers to enhance the convective heat exchange rates in SAHs. However, a few studies have analyzed SAHs using perforated absorbers in thermal aspects. This study introduces a novel SAH using multiple perforated absorbers and evaluates the transient dynamics and thermal efficiency of the new perforated SAH experimentally. To achieve this goal, the perforated SAH was constructed, and numerous sensors were utilized to monitor its heat dynamics and environmental conditions simultaneously.

The constructed SAH was mounted at 45^{o} of fixed tilt angle facing south, while the perforated absorbers were installed at 30^{o} to absorb the utmost incoming solar energy. This strategy provides pivotal flexibility in that the constructed SAH can be integrated with building walls, roofs, or inclined surfaces to meet required heating demands in commercial and residential buildings, especially in cases where there are space limitations in the

installation. Furthermore, using the perforated absorber is a more affordable method than the perforated artificial roughness since adding the perforated artificial roughness requires size, arrangement, and configuration optimizations. However, the perforated absorber is a simple, accessible technique that can be easily applied in SAHs.

EXPERIMENTAL METHOD

Experimental setup preparation

Figure 1 shows the experimental setup and the perforated SAH's schematics. The constructed SAH consists of medium-density fiberboards (MDFs), and its internal dimensions are 2.5 m × 0.4 m × 0.2 m. This collector uses a new absorber configuration formed from three inclined perforated metal plates installed at 30° to absorb the maximum incoming solar power. This SAH utilizes a 4 mm commercial glass cover placed at the top surface of the collector box to reduce radiant/convective heat losses.

The SAH was mounted at 45° to ease its installation on building walls, roofs, or inclined surfaces. A 50 W fan at the outlet opening produces desired flow rates. The flow rate was adjusted using a variable resistor to control fan speed. All gaps were sealed with silicon paste, avoiding air leakage.

Test conditions

The experiments were performed in Bam, Iran (29.0985° N, 58.3375° E), which has a 1061 m elevation from the sea level. The experiments began at 9:00, lasted 12 hours, and ended at 21:00 for several consecutive days in October 2022. The weather conditions were stable, clear, and sunny during experimental runs to ensure the same environmental conditions were created in the scenarios considered. The dynamics of the constructed SAH were analyzed at m_{air} = 0.012 kg/s and 0.024 kg/s (Reynolds number of 6500 and 13000). A data logger collected and recorded the acquired data provided by installed sensors every 5 minutes during experimental runs. These acquired data were utilized for further thermal analysis of the constructed perforated SAH.

Experimental setup sensors

Precise sensors have a crucial task in the accuracy of experimental data. Several sensors were employed to detect the transient dynamics of the perforated SAH and ambient conditions. These measured factors are ambient, outlet, and surface temperatures in conjunction with solar intensity. The measured data provide insight into how these parameters vary during experimental runs and affect the transient dynamics of the perforated SAH. Table 1 explains these measured data and installed sensor types.

(a)

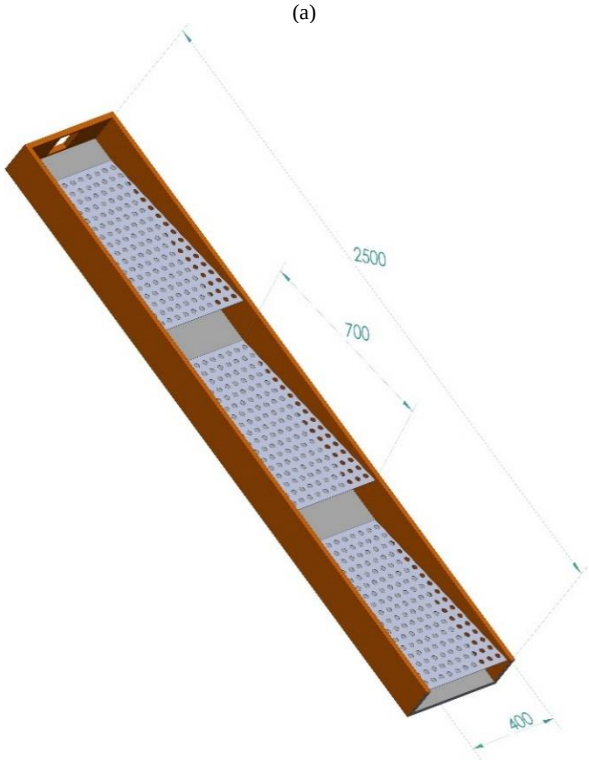

(b)

Figure 1. (a) Experimental setup component and (b) perforated SAH's schematics with dimensions in mm

Uncertainty analysis

Experimental measurements are subject to errors and uncertainties, affecting the quality of measurements. Error defines the difference between the measured and true value, while uncertainty estimates the magnitude of error, typically expressed in terms of a confidence interval within which the error lies. Since the current investigation utilizes an experimental approach, uncertainty and error analyses are crucial to judging the accuracy and preciseness of experimental data. The uncertainties of the main calculated factors are obtained as follows:

$$\frac{w_{\dot{m}_{air}}}{\dot{m}_{air}} = \left[\left(\frac{w_{T_{air}}}{T_{air}} \right)^2 + \left(\frac{w_{v_{in}}}{v_{in}} \right)^2 + \left(\frac{w_{P_{air}}}{P_{air}} \right)^2 \right]^{\frac{1}{2}} \quad (1)$$

$$\frac{w_{Q_{gain}}}{Q_{gain}} = \left[\left(\frac{w_{\dot{m}_{air}}}{\dot{m}_{air}} \right)^2 + \left(\frac{w_{\Delta T}}{\Delta T} \right)^2 \right]^{\frac{1}{2}} \quad (2)$$

$$\frac{w_{\eta}}{\eta_{I,Daily}} = \left[\left(\frac{w_{\dot{m}_{air}}}{\dot{m}_{air}} \right)^2 + \left(\frac{w_{\Delta T}}{\Delta T} \right)^2 + \left(\frac{w_{G}}{G} \right)^2 \right]^{\frac{1}{2}} \quad (3)$$

Here w_x is the uncertainties associated with the factor x. The accuracy and uncertainty of the critical measured and calculated factots are given in Table 2.

Energy analysis

Energy analysis provides a solid platform to compare and judge the performance of energy systems. The current study employs the first law of thermodynamics to perform energy analysis. This law determines how much energy source converts into accessible, valuable energy, which is employed to define thermal efficiency. Daily thermal efficiency is obtained as the ratio of total useful heat gain to total incoming solar energy as follows:

$$\eta_{I,daily} = \frac{\int_0^{\Delta t} \dot{m}_{air} c_{p,air} (T_{air,out} - T_{air,in}) dt}{\int_0^{\Delta t} A_c G dt} \quad (4)$$

Table 1. Measured data and installed sensor types

Measured parameter	Sensor type	Installation location
Inlet & outlet air temperatures	NTC thermistor	Inlet & outlet openings of perforated SAH
Perforated absorber temperature	NTC thermistor	Perforated absorber Plate surface
Ambient air temperature	Parto Negar TH202-485	Automatic weather station
Solar intensity	CMP3 Kipp&Zonen pyranometer	Automatic weather station
Air mass flow rate	TROTEC BA06 impeller anemometer	Inlet opening of perforated SAH

Table 2. Accuracy and standard uncertainty of main factors

Factor		Accuracy	Standard Uncertainty
Measured Factors	Inlet & Outlet Temperature	±0.5 °C	±5%
	Ambient Temperature	±0.5 °C	±5%
	Solar Irradiation	±10 W/m^2	±3%
	Wind Velocity	±0.01 m/s	±3%
	Inlet Air Velocity	±0.01 m/s	±5%
Calculated Factors	Mass Flow Rate	N.A.	±0.89%
	Heat Gain	N.A.	±3.24%
	Thermal Efficiency	N.A.	±4.54%

Here A_c is the total absorber surface area. $\dot{m}_{air}$ represents the mass flow rate, and $c_{p,air}$ defines the air specific heat. G is the solar intensity that hits the absorber plate. $T_{air,in}$ and $T_{air,out}$ represent the inlet and outlet temperatures.

RESULTS AND DISCUSSION

Perforations are a robust method to boost the convective heat exchange rate in SAHs. This study introduces a new SAH that uses three perforated inclined plates serving as the absorber to handle the weak inside the SAH. For this goal, a perforated SAH was fabricated, and its transient dynamics were monitored during experimental runs at m_{air} = 0.012 kg/s and 0.024 kg/s. Since environmental conditions are critical in the transient dynamics of the perforated SAH, crucial environmental parameters, such as ambient air temperature and solar intensity, were measured during experiments. Solar intensity determines the incoming solar thermal energy hitting the absorber and heating it, while the ambient temperature defines convective/radiant heat losses to the ambient.

Figure 2 depicts the measured environmental conditions. As shown in Figure 2, the solar intensity is nearly 500 W/m^2 at 9:00 and reaches 800 W/m^2 at noon. Then the solar intensity begins to reduce to approximately zero at sunset, 17:00. During this period, the ambient air temperature varies in a limited range. During the daytime, the ambient temperature varies between 28 °C to 31 °C; however, after sunset, the ambient air temperature suddenly reduces and reaches 22 °C. The solar intensity is high during the daytime to heat the absorber and flowing air. However, the solar intensity reaches below 200 W/m^2 after 15:00, which is insufficient for heating.

Figure 3 shows the measured perforated absorber temperature during experiments. As shown in Figure 3, the perforated absorber temperature strongly depends on the incoming solar intensity; in other words, the absorber temperature and solar intensity profiles have the same trend. The absorber temperature determines the highest potential available to heat the flowing air. The higher the absorber temperature, the higher the flowing air temperature.

The perforated absorber temperature reaches nearly 80 °C and 70 °C at m_{air} = 0.012 kg/s and 0.024 kg/s, which

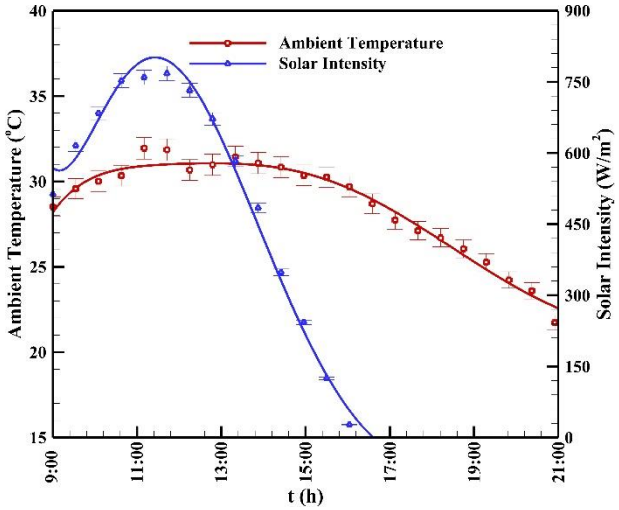

Figure 2. Measured ambient conditions

are high temperatures compared to the maximum ambient temperature, nearly 32 °C. The difference between the measured absorber temperatures in the two scenarios increases by increasing incoming solar energy. This difference reaches its maximum value, nearly 10 °C, at noon when the solar intensity has its maximum value. Then, the measured absorber temperatures and their difference reduce simultaneously with the solar intensity. The absorber temperature profiles are superimposed nearly at sunset when the solar intensity approaches zero, illustrating that when the incoming solar radiation is insufficient or absent, the perforated SAH dynamics are the same at dissimilar mass flow rates.

The absorber temperature reaches 20 °C at 21:00, 4 hours after sunset, which is nearly 2 °C lower than the ambient air temperature at the same time. This critical issue shows that the absorber plate exchanges radiant heat with its surroundings, especially the black sky, at night which causes the absorber temperature to reduce. This factor shows the importance of the radiant heat transfer mechanism at night that affects the dynamics of the collector.

The air mass flow rate significantly influences convection between the perforated absorber and the flowing air. Increasing the air mass flow rate increases the convection heat exchange rate. Hence more heat is extracted from the perforated absorber by the flowing air at a higher mass flow rate, and the absorber experiences a lower temperature. This subject is clearly represented in Figure 3 that in the scenario with m_{air} = 0.024 kg/s, the absorber attains a lower temperature than in the scenario with m_{air} = 0.012 kg/s.

Figure 4 depicts the measured outlet air temperature for the scenarios considered. Like the perforated absorber temperature profiles, the outlet air temperature profiles represent the same trend as the solar intensity profiles. Interestingly, the outlet temperature responds rapidly to the incoming solar radiation and reaches its maximum value at noon; then, it reduces approximately in a steep gradient to reach the ambient temperature at sunset. The system quickly responds to incoming solar radiation due to the low heat capacity of the system and lack of energy storage systems.

The outlet airflow temperature reaches 39 °C and 42 °C at m_{air} = 0.012 kg/s and 0.024 kg/s at noon and keeps within 90% of its maximum value for 2 hours. The perforation method causes the flowing air to exchange heat with the perforated absorber in an improved condition. Hence the flowing air gains more heat in contact with the perforated absorber and can maintain its temperature near the available peak temperature for extended periods. Then, the outlet temperature leaves the range within 90% of the available peak temperature at 15:00. The outlet airflow temperature profiles are superimposed nearly at 16:00 when the solar intensity reaches below 150 W/m^2, illustrating that the perforated SAH has the same heat dynamics at different air mass flow rates in the absence of the solar intensity.

The air mass flow rate is crucial in determining the convective exchange rate and the outlet airflow temperature. The high air mass flow reduces the air residence time in the SAH. Hence the convection period reduces, and this subject results in decreasing the outlet temperature.

Figure 5 shows the hourly heat gains in the considered scenarios during experiments. As shown in Figure 5, the hourly heat gains enhance during the daytime by increasing the outlet air temperature and solar intensity. Heat gains reach their peak value between 12:00 and 14:00 in both scenarios, and the heating process continues in the afternoon; however, the accumulated heat gains are negligible near sunset. Enhancing the air mass flow rate increases the hourly heat gains, even though the

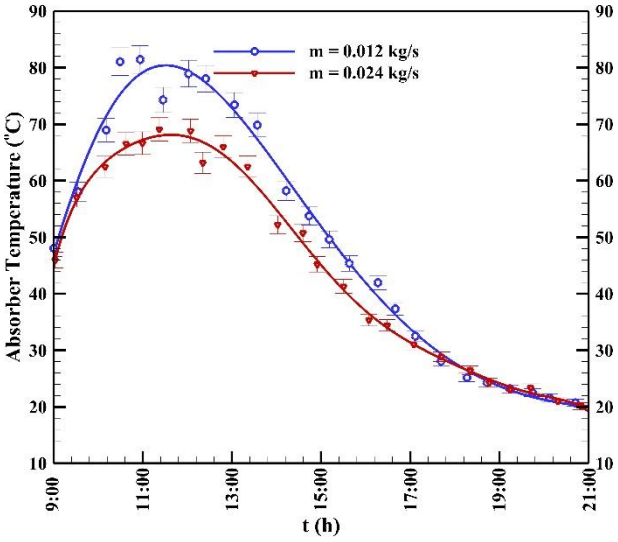

Figure 3. Measured perforated absorber temperature

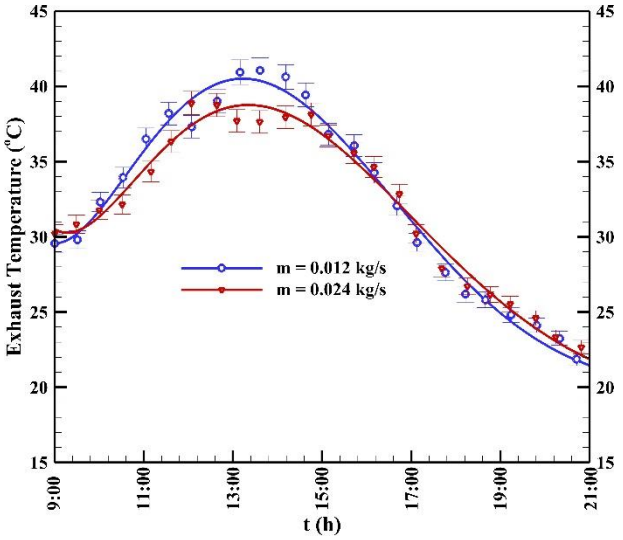

Figure 4. Measured outlet air temperature

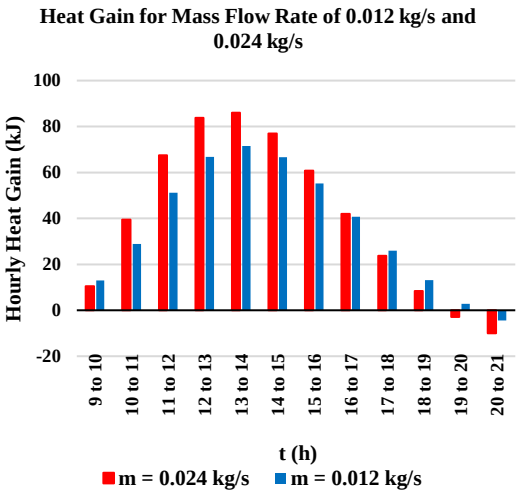

Figure 5. Hourly heat gains

increment in the accumulated heat gains is small. In other words, the peak values of the accumulated heat gains increase by only 21.1% by enhancing the mass flow rate by two times.

During night hours, the accumulated heat gains reduce to negative values, which means that the flowing air is cooled by passing through the collector. The absorber temperature reduces during night hours because of the radiant exchange with the black sky. This issue causes the flowing air to lose its heat content due to exchanging heat with the cold absorber.

Table 3 represents the obtained thermal efficiency and total heat gains of the perforated SAH in the scenarios considered. During experimental runs, the perforated SAH collects 431.15 kJ and 486.17 kJ at m_{air} = 0.012 kg/s and 0.024 kg/s. The calculated thermal efficiencies reveal that using the perforation method significantly improves the efficiency of the perforated SAH compared to conventional SAHs. Using this method results in reaching the efficiency of 82.65%, which is a high value for SAHs. Furthermore, by enhancing the mass flow rate by two times, the efficiency increases by nearly 12.75%. The current study illustrates that using the perforation method in SAH significantly improves thermal efficiency.

Table 4 represents a comprehensive comparison between the thermal efficiencies of perforated SAHs and conventional SAHs using other thermal enhancement techniques. SAHs utilize numerous techniques to improve thermal efficiency; however, their thermal efficiencies are usually in a range of 25 to 78%, depending on configurations and operational/ environmental conditions [2, 4, 5]. As seen in Table 4, the perforation method helps SAHs reach a high thermal efficiency compared to other techniques.

Table 3. Calculated thermal efficiency and heat gains of perforated SAH

Scenario	Thermal efficiency (%)	Total heat gain (kJ)
$\dot{m} = 0.012\ kg/s$	73.30	431.15
$\dot{m} = 0.024\ kg/s$	82.65	486.17

Table 4. A comprehensive comparison between the current and recent studies

Reference	SAH type and strategy	Air mass flow rate/Reynolds number		Daily thermal efficiency
		$\dot{m}$ (kg/s)	Re	
Kabeel et al. [4], Arunkumar et al. [5], Singh et al. [2]	Conventional SAH/SAH using thermal enhancement techniques	0.005 to 0.04	5000 to 20000	25% to 75%
Vaziri et al. [9]	SAHs with perforated metal and plexiglass top covers	0.017 to 0.036	N.A.	85%
Mahmood [19]	Double-pass unglazed SAH with perforated plate and wire mesh layers	0.003 to 0.018	N.A.	86%
Shetty et al. [21]	SAH with perforated circular absorber plate	N.A.	9000 to 15000	75.55%
Arunkumar et al. [22, 23]	SAH with rectangular perforated duct inserts	N.A.	3000 to 18000	83.01%
Current study	SAH with inclined perforated absorber plates	0.012 and 0.024	6500 and 13000	82.65%

CONCLUSION

Conventional SAHs have an inherent drawback: the convection heat mechanism is weak in these solar thermal collectors. This study analyzes a new approach to handle this problem in an effective, affordable method. A new SAH using three inclined perforated absorber plates has been introduced to this aim. This perforated SAH has been analyzed experimentally under field conditions in two scenarios, including at m_{air} = 0.012 kg/s and 0.024 kg/s. The obtained experimental data illustrate that the constructed perforated SAH has a higher thermal efficiency, nearly 82.65%, than conventional SAH, which means the perforation method can increase thermal efficiency. In brief, the obtained results can be given as follows:

- The perforated absorber temperature reaches nearly 80 ^{o}C and 70 ^{o}C at m_{air} = 0.012 kg/s and 0.024 kg/s, which are high temperatures compared to the maximum ambient temperature, nearly 32 ^{o}C.
- The difference seen between the absorber temperature profiles increases by increasing the solar intensity and vice versa. This difference reaches its maximum value, nearly 10 ^{o}C, at noon when the solar intensity has its peak value.
- The absorber temperature profiles are superimposed nearly at sunset, illustrating that when the incoming solar power is insufficient, the perforated SAH dynamics are the same at dissimilar mass flow rates.
- The outlet air and absorber temperatures respond rapidly to the incoming solar radiation and reach their maximum values at noon; then, they reduce approximately in a steep gradient in the afternoon.
- The outlet airflow temperature reaches 39 ^{o}C and 42 ^{o}C at m_{air} = 0.012 kg/s and 0.024 kg/s, respectively, at noon and maintains within 90% of its maximum value for 2 hours.
- The perforation method improves the heat convection mechanism. This issue results in the outlet air temperature maintaining near the peak temperature for extended periods.
- The air mass flow rate influences the heat dynamics of the perforated SAH. The higher the air mass flow rate, the lower the outlet air temperature. The maximum outlet air temperature reduces by nearly 5 ^{o}C by increasing m_{air} from 0.012 kg/s to 0.024 kg/s.
- The perforated SAH collects 431.15 kJ and 486.17 kJ at m_{air} = 0.012 kg/s and 0.024 kg/s during experimental runs.
- The peak values of the accumulated heat gains enhance by 21.1% by increasing m_{air} by two times.
- Using this method results in reaching the efficiency of 82.65%, which is a high value for SAHs. Furthermore, by increasing m_{air} by two times, the thermal efficiency improves by nearly 12.75%.

ACKNOWLEDGEMENT

The authors are thankful to Higher Education Complex of Bam, Iran.

CONFLICT OF INTEREST

The authors declare no conflict of interests.

REFERENCES

1. Farzan, H., 2019. The study of thermostat impact on energy consumption in a residential building by using TRNSYS, *Journal of Renewable Energy and Environment*, 6(1), pp. 15-20. Doi: 10.30501/jree.2019.95531
2. Singh, V. P., Jain, S., Karn, A., Kumar, A., Dwivedi, G., Meena, C. S., Dutt, N. and Ghosh, A., 2022. Recent developments and advancements in solar air heaters: a detailed review, *Sustainability*, 14(19), pp. 12149. Doi: 10.3390/su141912149
3. Ameri, M., Farzan, H. and Nobari, M., 2021. Evaluation of different glazing materials, strategies, and configurations in flat plate collectors using glass and acrylic covers: An experimental assessment, *Iranian (Iranica) Journal of Energy & Environment*, 12(4), pp. 297-306. Doi: 10.5829/ijee.2021.12.04.03
4. Kabeel, A. E., Hamed, M. H., Omara, Z. and Kandeal, A., 2017. Solar air heaters: Design configurations, improvement methods and applications–A detailed review, *Renewable and Sustainable Energy Reviews*, 70, pp. 1189-1206. Doi: 10.1016/j.rser.2016.12.021
5. Arunkumar, H., Karanth, K. V. and Kumar, S., 2020. Review on the design modifications of a solar air heater for improvement in the thermal performance, *Sustainable Energy Technologies and Assessments*, 39, pp. 100685. Doi: 10.1016/j.seta.2020.100685
6. Saravanan, A., Murugan, M., Reddy, M. S., Ranjit, P., Elumalai, P., Kumar, P. and Sree, S. R., 2021. Thermo-hydraulic performance of a solar air heater with staggered C-shape finned absorber plate, *International Journal of Thermal Sciences*, 168, pp. 107068. Doi: 10.1016/j.ijthermalsci.2021.107068
7. Singh, V. P., Jain, S. and Gupta, J., 2022. Performance assessment of double-pass parallel flow solar air heater with perforated multi-V ribs roughness—Part B, *Experimental Heat Transfer*, 35(7), pp. 1-18. Doi: 10.1080/08916152.2021.2019147
8. Singh, V. P., Jain, S. and Gupta, J., 2022. Analysis of the effect of variation in open area ratio in perforated multi-V rib roughened single pass solar air heater-Part A, *Energy Sources, Part A: Recovery, Utilization, and Environmental Effects*, pp. 1-21. Doi: 10.1080/15567036.2022.2029976
9. Vaziri, R., İlkan, M. and Egelioglu, F., 2015. Experimental performance of perforated glazed solar air heaters and unglazed transpired solar air heater, *Solar Energy*, 119, pp. 251-260. Doi: 10.1016/j.solener.2015.06.043
10. Skullong, S., Promthaisong, P., Promvonge, P., Thianpong, C. and Pimsarn, M., 2018. Thermal performance in solar air heater with perforated-winglet-type vortex generator, *Solar Energy*, 170, pp. 1101-1117. Doi: 10.1016/j.solener.2018.05.093
11. Faujdar, S. and Agrawal, M., 2021. Computational fluid dynamics based numerical study to determine the performance of triangular solar air heater duct having perforated baffles in V-down pattern mounted underneath absorber plate, *Solar Energy*, 228, pp. 235-252. Doi: 10.1016/j.solener.2021.09.006

12. Jain, S. K., Misra, R., Kumar, A. and Agrawal, G. D., 2022. Thermal performance investigation of a solar air heater having discrete V-shaped perforated baffles, *International Journal of Ambient Energy*, 43(1), pp. 243-251. Doi: 10.1080/01430750.2019.1636874
13. Hassan, H., Yousef, M. S. and Abo-Elfadl, S., 2021. Energy, exergy, economic and environmental assessment of double pass V-corrugated-perforated finned solar air heater at different air mass ratios, *Sustainable Energy Technologies and Assessments*, 43, pp. 100936. Doi: 10.1016/j.seta.2020.100936
14. Pandey, R. and Kumar, M., 2021. Efficiencies assessment of an indoor designed solar air heater characterized by V baffle blocks having staggered racetrack-shaped perforation geometry, *Sustainable Energy Technologies and Assessments*, 47, pp. 101362. Doi: 10.1080/15435075.2022.2083916
15. Khanlari, A., Tuncer, A. D., Sözen, A., Aytaç, İ., Çiftçi, E. and Variyenli, H. İ., 2022. Energy and exergy analysis of a vertical solar air heater with nano-enhanced absorber coating and perforated baffles, *Renewable Energy*, 187, pp. 586-602. Doi: 10.1016/j.renene.2022.01.074
16. Tandel, H. U. and Modi, K. V., 2022. Experimental assessment of double-pass solar air heater by incorporating perforated baffles and solar water heating system, *Renewable Energy*, 183, pp. 385-405. Doi: 10.1016/j.renene.2021.10.087
17. Dutta, P., Goswami, P., Sharma, A., Dutta, P. P. and Baruah, M., 2022. Computational Performance Analysis of the Perforated and Flat Plates Double Pass Solar Air Heaters, *Advances in Thermofluids and Renewable Energy*: Springer, pp. 549-561. Doi: 10.1007/978-981-16-3497-0_44
18. Bhattacharyya, S., Pathak, M., Sharifpur, M., Chamoli, S. and Ewim, D. R., 2021. Heat transfer and exergy analysis of solar air heater tube with helical corrugation and perforated circular disc inserts, *Journal of Thermal Analysis and Calorimetry*, 145(3), pp. 1019-1034. Doi: 10.1007/s10973-020-10215-x
19. Jasim Mahmood, A., 2020. Thermal evaluation of a double-pass unglazed solar air heater with perforated plate and wire mesh layers, *Sustainability*, 12(9), pp. 3619. Doi: 10.3390/su12093619
20. Shetty, S. P., Nayak, S., Kumar, S. and Karanth, K. V., 2021. Thermo-hydraulic performance prediction of a solar air heater with circular perforated absorber plate using Artificial Neural Network, *Thermal Science and Engineering Progress*, 23, pp. 100886. Doi: 10.1016/j.tsep.2021.100886
21. Shetty, S. P., Paineni, A., Kande, M., Madhwesh, N., Sharma, N. Y. and Karanth, K. V., 2020. Experimental investigations on a cross flow solar air heater having perforated circular absorber plate for thermal performance augmentation, *Solar Energy*, 197, pp. 254-265. Doi: 10.1016/j.solener.2020.01.005
22. Arunkumar, H., Kumar, S. and Karanth, K. V., 2021. Experimental study on thermo-hydraulic performance of a solar air heater with rectangular perforated duct inserts, *Solar Energy*, 227, pp. 179-189. Doi: 0.1016/j.solener.2021.09.005
23. Arunkumar, H., Kumar, S. and Karanth, K. V., 2022. Performance enhancement of a solar air heater using rectangular perforated duct inserts, *Thermal Science and Engineering Progress*, 34, pp. 101404. Doi: 10.1016/j.tsep.2022.101404

Persian Abstract

چکیده

گرمکن‌های هوایی خورشیدی دارای یک ایراد ذاتی شامل انتقال حرارت جابجایی ضعیف بین جریان هوای عبوری و صفحه جاذب هستند. استفاده از صفحات مشبک یک روش ساده برای بهبود جابجایی در مسائل انتقال حرارت است. مطالعه حاضر با استفاده رویکرد تجربی نوع جدیدی از گرمکن‌های هوایی برای حل این ایراد ذاتی معرفی و بررسی می‌کند.این گرمکن هوایی از سه صفحه سوراخ دار مایل به عنوان صفحه جاذب استفاده می‌کند. دو سناریو برای بررسی و تحلیل دینامیک و راندمان حرارتی گرمکن هوایی، شامل بررسی تجربی گرمکن در دبی‌های جرمی ۰/۰۱۲ kg/s و ۰/۰۲۴ kg/s، در نظر گرفته شده است. حسگرهای متفاوتی برای نظارت بر رفتار دینامیکی گرمکن و شرایط محیطی استفاده شده است و آزمایش‌ها برای چند روز متوالی و به مدت ۱۲ ساعت در ماه آبان سال ۲۰۲۲ انجام پذیرفته است. نتایج آزمایش نشان می‌دهند استفاده از صفحه‌های مشبک راندمان حرارتی گرمکن هوایی را به مقدار زیادی نسبت به گرمکن‌های هوایی متداول افزایش می‌دهد. راندمان روزانه گرمکن هوایی ساخته شده به مقدار ۷۳/۳۰٪ و ۸۲/۶۵٪ و مقدار دمای هوای خروجی به عدد ۳۹°C و ۴۲°C در هنگام ظهر می‌رسد. دمای هوای خروجی از گرمکن هوایی در محدوده ۹۰٪ دمای هوای بیشینه خروجی به مدت ۲ ساعت باقی می‌ماند. بهبود انتقال حرارت جابجایی در گرمکن هوایی با استفاده از جاذب مشبک سبب می‌گردد، جریان هوای عبوری از کلکتور انرژی حرارتی صفحات جاذب را به شکل موثری جذب نماید. از این رو، گرمکن هوایی مشبک می‌تواند یک جریان هوا با دمای پایدار نزدیک به دمای بیشینه را برای مدت طولانی‌تری تولید نماید. در نتیجه، استفاده از جاذب مشبک یک راه حل موثر و ساده برای افزایش راندمان حرارتی گرمکن‌های هوایی خورشیدی است.